Materials Today Communications 26 (2021) 102120

Contents lists available at ScienceDirect

Materials Today Communications

journal homepage: www.elsevier.com/locate/mtcomm

Tuning the electrical performance of solution-processed In_2O_3TFTs by low-temperature with HfO_2-PVP hybrid dielectric

M.G. Syamala Rao [a,*], J. Meza-Arroyo [a], K. Chandra Sekhar Reddy [a], Lakshmi N.S. Murthy [b], M. S. de Urquijo-Ventura [a], F. Garibay-Martínez [a], Julia W.P Hsu [b], R. Ramirez-Bon [a]

[a] Centro de Investigación y de Estudios Avanzados del IPN, Unidad Querétaro, Apdo, Postal 1-798, 76001 Querétaro, Querétaro, Mexico
[b] Department of Materials Science and Engineering, The University of Texas at Dallas, 800 West Campbell Road, Richardson, 75080, Texas, United States

ARTICLE INFO

Keywords:
HfO_2-PVP
Hybrid dielectric
Low-temperature
Solution process
In_2O_3 TFT

ABSTRACT

Here in, we investigated the solution-processed and hysteresis-free indium oxide (In_2O_3) thin-film transistors (TFTs) fabricated with hafnium oxide-poly(vinyl)phenol (HfO_2-PVP) hybrid thin film as gate dielectric by a low temperature sol-gel method. The hybrid dielectric thin film exhibits unique dielectric properties of a low leakage current density of 1.2×10^{-8} A/cm^2, gate areal capacitance of 44.4 nF/cm^2 and a dielectric constant (k) of 6.5 at 1 kHz. In addition, the hybrid films show a high-quality homogeneous and pin-hole free surface with a low surface roughness (R_q) of 0.75-nm and display a low surface energy of 36.7 mJ/m^2 with hydrophobic behavior. This dielectric material is then used used in In_2O_3 TFTs as the gate insulator. Here, the In_2O_3 semiconductor as the channel layer is examined at 200 °C and 230 °C temperatures for TFT characteristics. The final TFT device fabricated at 230 °C showed much improved electrical performance with the mobility (μ_{sat}) of 2.6 cm^2/V.s, I_{on}/I_{off} ratio of 10^5, subthreshold swing (SS) of 330 mV/dec, threshold voltage (V_T) of 0.1 V at a low operating voltages because of a better interface between dielectric and semiconductor with fewer charge carriers traps. This study could be an effective approach for the next generation of all-solution fabrication of TFTs that could play a vital role in optoelectronics applications.

1. Introduction

The solution processes advance as an alternative to conventional thin films physical deposition methods, and highly encouraging the open up of new possibilities in the fabrication of large-scale and low-cost electronic devices. Recently, the solution processes have triggered the fabrication of high-performance metal-oxide thin film transistors (TFTs) exclusively for applications in the next generation electronic devices such as high definition flexible displays, organic light-emitting diodes (OLEDs) and many others [1–3]. In this respect, with the increasing interest on high-performance and low-cost TFTs, there is a current intensive searching for high-quality semiconductors and dielectrics materials processed at low temperatures for the next generation of flexible TFTs applications.

Recently, solution-processed metal-oxide TFTs have been achieved with a variety of n-type oxide semiconductor materials instigated by indium gallium zinc oxide (a-IGZO), zinc oxide (ZnO), indium zinc oxide (IZO) and indium oxide (In_2O_3) as channel layers [4–7]. As a result, remarkable advantages like easy processability, inherent scalability and high mobility devices have been demonstrated by various solution-based methods such as combustion synthesis and sol-gel [8,9]. While substantial progress has been made through the solution process of these semiconductors as channel layers for TFTs, particular focus has been recognized on In_2O_3, due mainly to its exceptionally low deposition processing temperature (< 250 °C) [10,11]. However, most solution processed In_2O_3 TFT devices, which are usually manufactured with thermally grown SiO_2 as the dielectric gate, perform poor drain currents [12,13]. This is in part due to the SiO_2 low dielectric constant and makes necessary the increase to higher operating voltages to achieve higher drain currents in the channel layer [8]. Therefore, for the completion of fully solution fabrication of low power consumption metal oxide TFTs, it is also obligatory to develop solution-processed dielectrics with enhanced properties.

Unlike the excellent research on semiconductor materials for TFT applications, the investigation of dielectric materials by low temperature solution process has not yet been well advanced. The dielectric gate

* Corresponding author.
E-mail address: mullapudi.gouri@gmail.com (M.G.S. Rao).

https://doi.org/10.1016/j.mtcomm.2021.102120
Received 11 January 2021; Accepted 3 February 2021
Available online 11 February 2021

layer is a critical component of TFTs, which properties have a strong impact on the field effect mobility and other important electrical parameters of the device. For flexible TFTs, the conventional SiO_2 dielectric gate material is discarded because its high processing temperature and low dielectric constant (3.9) [14]. To overcome this, research on dielectric materials with high dielectric constants (k>20) increased rapidly in the last years. Among the foremost high-k dielectric materials with the chance to be processed in solution are HfO_2, ZrO_2 and Al_2O_3 [15–17]. Moreover, the incorporation of these high-k dielectrics in oxide TFTs has an excellent compatibility with solution processed oxide semiconductors in device fabrication by complete solution processes. There are simple chemical routes to achieve semiconductor channels forming smooth interfaces, limiting the density of traps and leading to high electrical performance at low operating voltages [18]. HfO_2 is among the leading high-k dielectrics materials, which has been widely studied and applied in many devices because of its properties such as high capacitance and dielectric constant (k∼15−30), large band gap (>6 eV), low leakage current density, high electrical break down strength, and importantly, good chemical resistance with a lot of substrates [19,20]. Apart from its unique dielectric performance, the major disadvantage of HfO_2 is the high thermal annealing temperature (> 350 °C) required for densifying the thin films and then achieve the excellent insulating properties. However, despite the excellent dielectric properties of HfO_2 thin films annealed at high temperatures, their brittle mechanical behaviour, due to the high young modules, limit them for potential flexible electronic applications [21,22].

Recently, several research groups are focusing on the development of new dielectric materials processed at low temperatures (< 200 °C) as compared to ceramic dielectrics for TFT applications. In this consequence, organic dielectric polymers such as polyvinyl phenol (PVP), polyvinyl alcohol (PVA), polyvinylidene difluoride (PVDF) and its copolymers, and cyanide-based polymers have gained rapid attention due to their relatively high dielectric constants (k ≥ 5) and excellent insulating properties [23–26]. Additionally, they can be incorporated as gate dielectrics with simple solution processes at low fabrication-cost and high mechanical flexibility. However, most of these dielectric polymers are used for organic thin-film transistors (OTFTs) in combination with p or n-type organic semiconductors [27]. OTFTs emphasize adequate electrical performance in both cases, including low operating voltages [25,27]. Although organic dielectrics grow rapidly but limited for OTFTs fabrication, there are very few reports about organic dielectrics for high performance semiconductor oxides TFTs. This is due to their inferior dielectric performance such as degradation and reliability as compared to inorganic dielectrics in semiconductor oxide TFTs. Moreover, poor dielectric/semiconductor interface properties are also drawbacks of the dielectric polymers for the metal oxide TFTs fabrication [28]. To overcome some of these issues, the dielectric polymers have been modified to enhance their properties. For example, poly (4-vinylphenol) (PVP) crosslinked with poly (melamine-*co*-formaldehyde) (PMF) make it to c-PVP dielectric polymer exhibits superior insulating characteristics and it is compatible with most of the inorganic semiconductors. Recently, c-PVP gate dielectric layers are applied in the fabrication of many semiconductor oxide based TFTs [29,30]. In a hybrid approach, the organic dielectric layer is commonly covered with a high-k inorganic dielectric layer to improve the interfacial properties with the inorganic semiconductor channels and to avoid the dielectric polymer degradation.

Recently, inorganic-organic hybrid materials are being presented as a new class of gate dielectric layers for the TFTs fabrication. These dielectric materials are feasible alternatives to overcome some of the issues of the organic dielectrics. A mix of a high-k inorganic dielectric and an organic dielectric polymer generally constitutes the hybrid dielectric materials. This approach takes advantage of both types of materials to improve the properties of the hybrid materials as compared to one or the other constituting phase. Therefore, it is possible to achieve dielectric materials with high dielectric constant (inorganic contribution) keeping some mechanical flexibility (organic contribution) even at low processing temperatures below 200 °C [31–35]. This is because solution processes at low temperature can obtain the hybrid materials. These solution-processed hybrid dielectrics exhibit low leakage current density with excellent morphological properties such as smooth surface for better interface properties with fewer charge carrier traps [36]. Their surface energy is typically low with hydrophobic behavior appropriate for the deposition of the semiconductor channel by solution processes. For these reasons, hybrid dielectric materials can extend the applications of flexible electronics devices, especially those related with TFTs [34]. However, although the idea of combining two materials with complementary properties is straightforward, the synthesis of hybrid materials with synergistic properties requires the proper bonding between the organic and inorganic phases, which is still a challenging task.

Among high-k inorganic oxide dielectrics, HfO_2 stands out due to its remarkable dielectric properties. It is currently one of the most widely applied dielectric material in metal-oxide TFTs. Nevertheless, the high processing temperature, necessary to densify the dielectric gate layers and their brittle behaviour limit to extend HfO_2 as gate dielectric in flexible devices. In our recent work, we successfully combined HfO_2 as the inorganic phase with PMMA as the organic one in a HfO_2 -PMMA hybrid dielectric material. The dielectric layers of this hybrid material deposited at low temperature performed very well in ZnO-based TFTs [37]. On the other hand, PVP (poly (vinylphenol)) is a dielectric polymer widely employed in organic TFTs (OTFTs) [25]. The main advantage of this organic dielectric over PMMA is its higher dielectric constant of k∼5. Thus, PVP is a dielectric polymer very convenient to combine with high-k inorganic dielectric in hybrid dielectric materials. The PVP-based hybrid materials have been much less studied than the PMMA-based ones. There are some recent works about PVP hybrid dielectrics in the form of bilayers and polymer nanocomposites with application to dielectric gates in inorganic semiconductor devices [38,39]. We have synthesized PVP, PVP-SiO_2 and PVP-TiO_2 dielectric gate layers at low temperature and successfully applied them to the fabrication of TFTs with inorganic CdS semiconductor channel layers [29,36].

In this work we propose and develop a novel hybrid dielectric material based on hafnium oxide (HfO_2) combined with cross-linked PVP polymer to acquire HfO_2-PVP hybrid thin films with excellent insulating properties for dielectric gate applications to metal oxide TFTs. The HfO_2-PVP hybrid dielectric films were deposited by the sol-gel spin-coating process and annealed at 200 °C to cross-link the phases. The smooth and pinhole-free hybrid thin films exhibited outstanding dielectric properties such as low leakage current density, respectable capacitance with good dielectric constant (k). In addition, the hybrid thin films surface had hydrophobic behavior, which implies low surface free energy, and is ideal for the deposition in solution of In_2O_3 semiconductor channel layer. This way, we report the fully solution processed metal oxide TFTs, fabricated on ITO-coated glass substrates at low annealing temperatures < 230 °C, with the incorporation of HfO_2-PVP hybrid thin film as gate dielectric and In_2O_3 as active channel. Thus, the fully solution fabricated In_2O_3 TFTs had enhanced electrical performance with saturation mobility of 2.6 cm^2/V.s, threshold voltage of 0.1 V, subthreshold swing of 330 mV/dec and current $I_{on/off}$ ratio of 10^5.

2. Experimental section

2.1. Materials synthesis

For the TFTs fabrication, both dielectric and semiconductor layers were deposited by solution process at low temperature. For the synthesis of the inorganic precursor solution, 0.2 M $HfCl_4$ was dissolved in 2-methoxyethanol to obtain a transparent solution. After 15 min of vigorous stirring, 0.1 M HNO_3 and 0.1 M DI water were added continuously into this solution to encourage the sol-gel hydrolysis and condensation reactions. The final inorganic solution was constantly

stirred for 4 h at 60 °C. Then, the polymer PVP solution was prepared from its precursor of 10 mM PVP (M.W~11,000), which was dissolved into propylene glycol monomethyl ether acetate (PGMEA) solvent and subsequently stirred for 30 min to obtain a homogeneous solution. Later, polymelamine-*co*-formaldehyde (PMF) was mixed into this solution as a crosslinking mediator to reduce the phenolic groups (−OH) that are included in PVP. Finally, the crosslinked PVP (PMF-PVP) solution was stirred for 6 h at room temperature. To make the hybrid solution, both individual inorganic and organic solutions were mixed with a different % volume ratios of 80/20, 60/40 and 20/80 and the final hybrid solutions were stirred for 3 h to complete the crosslinking of the hybrid solution. The hybrid thin films were deposited by spin coating process from the hybrid precursor solutions. The scheme with the complete hybrid thin films deposition process is shown in Fig. 1. For the preparation of In_2O_3 semiconductor solution, 0.1 M $In(NO_3)$ x.H_2O precursor was dissolved in 2-methoxy ethanol followed by 0.1 M acetylacetone and ammonium hydroxide (NH_4OH) was added to stabilize the solution and the final solution was vigorously stirred for the overnight at room temperature. Both hybrid and semiconductor solutions were filtered through 0.45 μm PTFE syringe filters before the deposition of thin films.

2.2. MIM and TFT devices fabrication

Metal-Insulator-Metal (MIM) capacitor device structures were fabricated on cleaned ITO-coated glass substrates to examine the dielectric properties of HfO_2-PVP hybrid thin films. For this, 0.5 mL of hybrid precursor sol was dispersed on the top of the ITO-coated substrate and deposited by spin coating process with a spinning speed of 3000 rpm for 30 s under ambient environment. The deposited wet gel thin films were immediately placed on a hot plate at 150 °C to remove the organic residuals from their surface, and then baked at 200 °C for 3 h to complete the crosslinking procedure in a conventional oven. Finally, the achieved 132-nm thick, smooth and homogeneous hybrid thin films were utilized as dielectric for MIM devices, for which gold contacts were deposited on this hybrid surface by shadow mask process with 0.02 cm^2 area. Similarly, for the fabrication of In_2O_3 TFTs on ITO-coated glass as bottom gate substrate, the In_2O_3 semiconductor thin films were deposited on the top of the hybrid dielectric through spin coating process with a spinning speed of 3000 rpm for 30 s, followed by two-step annealing process. First, the films were pre-baked on a hot plate at 80 °C for 1 min and then exposed under UV-ozone light for 10 min and this step was repeated twice for the required thickness of ~10−15 nm. Second, annealed at two different temperatures of 200 °C and 230 °C for 20 min on the same hot plate to get homogeneous transparent In_2O_3 thin films. Finally, aluminum (Al) top contacts were evaporated to pattern the source and drain contacts by using a conventional shadow mask technique.

2.3. Thin film and devices characterization

The structural characterization of the HfO_2-PVP hybrid thin-films was first scrutinized by the thermogravimetric (TGA) (TA SDT 421Q600) technique to inspect their thermal decomposition. For this, the produced wet gel hybrid precursor solutions were initially dried at 70 °C to remove all organic solvents. Finally, the obtained dehydrated hybrid powders were annealed at 200 °C for 3 h. The hybrid thin films were characterized by FTIR (PerkinElmer spectrometer, spectrum GX) analysis to identify the chemical functional groups forming the hybrid network. Similarly, the XPS (Intercovamex 110) technique was employed to corroborate the chemical states of the elements in the hybrid films. The hybrid dielectric properties were determined from capacitance vs voltage (*C-V*) and leakage current vs voltage (*I-V*) measurements in ambient conditions by using LCR meter (HP4284A) and Keithley semiconductor analyzer (Keithley 4200), respectively. The hybrid dielectric layer roughness was measured by AFM, and the morphology and cross-section of dielectric layer were characterized by FESEM. On the other hand, the spin deposited In_2O_3 semiconductor channel layer roughness was measured by AFM. The In_2O_3–based TFT device electrical parameters were analyzed from current versus voltage measurements by using a Keithley semiconductor analyzer (Keithley 4200) in dark conditions.

3. Results and discussion

3.1. Chemical structural characterization of hybrid films

Fig. 1 depicts the synthesis route for the deposition of inorganic-organic HfO_2-PVP thin films well crosslinked with PMF molecules. The spin coated hybrid thin films were prepared from its precursor solutions to make robust hybrid thin films enlaced with strong covalent bonds. Before utilizing these films as dielectric layers, they were characterized by Fourier transform infrared spectroscopy (FTIR) spectroscopy and X-ray photoelectron spectroscopy (XPS) to identify the presence of hydroxyl groups, as well as the chemical bonds and their properties to optimize the crosslinking process of the hybrid thin films.

Fig. 2 displays the FTIR spectrum of the hybrid thin film. The low

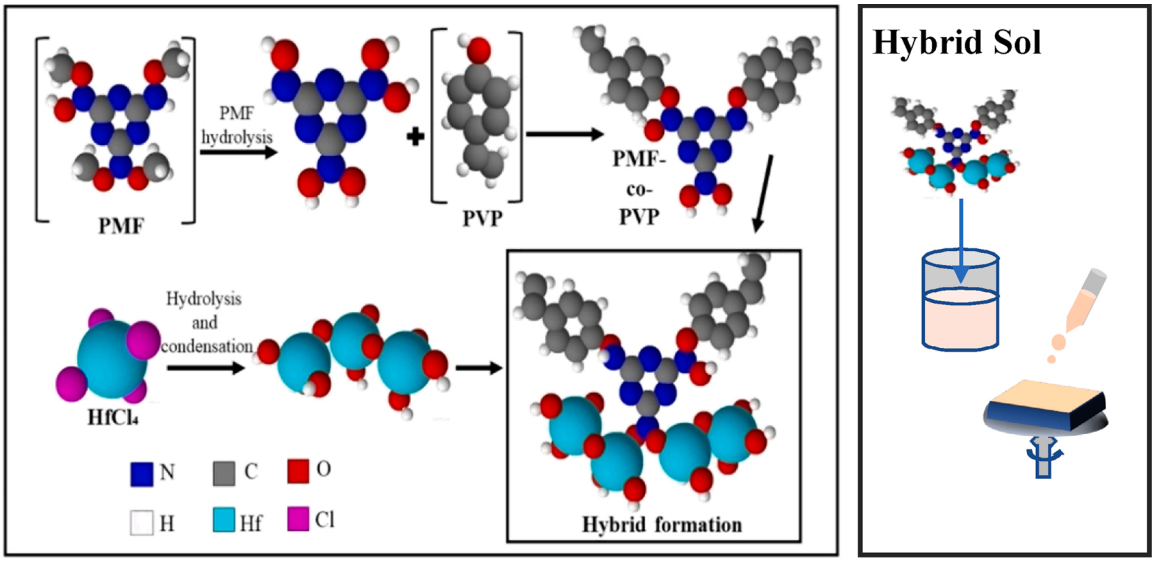

Fig. 1. Schematic of the deposition route of HfO_2-PVP hybrid dielectric thin films.

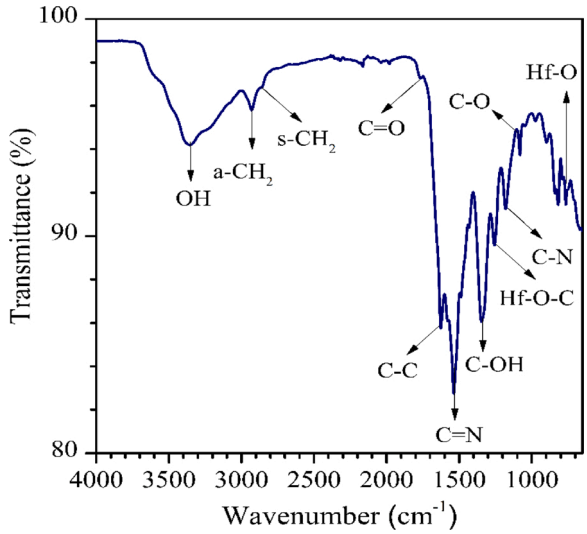

Fig. 2. FTIR spectrum of the hybrid HfO_2-PVP dielectric thin film.

intensity absorption band observed at 3375 cm^{-1} is associated to the −OH stretching vibration modes, this might be expected due to the presence Hf−OH groups from the incomplete condensation of the inorganic phase during the sol-gel synthesis and the c-PVP ring bonding with inorganic hafnium oxide whereas crosslinking process takes place in the hybrid network [25,27]. The latter might be due to insufficient crosslinking between the hybrid phases resulting in unreacted hydroxyl groups. The band at 2927 cm^{-1} and 2863 cm^{-1} are correlated to the $-CH_2$ stretching vibrations in the c-PVP polymer [34]. The low intensity shoulder observed at 1759 cm^{-1} is assigned to carbonyl C═O stretching vibration modes [25] and the peaks at 1624 cm^{-1} and 1083 cm^{-1} are assigned to the stretching vibrations of C—C and C—O groups. Additionally, the sharp narrow peak at 1344 cm^{-1} is associated to C—OH bending vibrations and all of these carbon peaks reveal the presence of phenolic PVP polymer in the hybrid thin film [36]. On the other hand, the sharp narrow peak at 1534 cm^{-1} and the small peak at 1173 cm^{-1} are related to stretching vibrations of C═N and C—N groups, which are characteristic groups of the crosslinking PMF molecule [36,40]. The peak at 1254 cm^{-1}, which comes from vibration modes of Hf-O-C is revealing that strong covalent chemical bond formed between the inorganic HfO_2 and the PVP polymer [41]. This confirms the successful homogeneous hybrid thin film formation, with organic and inorganic phases strongly bonded. Finally, the small peak at 759 cm^{-1} was attributed to the inorganic HfO_2 phase in the hybrid material [41]. Therefore, from the FTIR results it is clearly suggested a great evidence for the successful formation of HfO_2-PVP hybrid thin film via strong covalent bonds.

The XPS technique was employed to investigate more deeply the chemical binding states between the elements in the HfO_2-PVP hybrid thin films. The core level XPS spectra for Hf 4f, O 1s, C 1s and N 1s, are shown in Fig. 3 a), b), c) and d), respectively. The Hf 4f spectrum in Fig. 3 (a) can be deconvoluted into two core splitting peaks at binding energies of 18.5 eV and 20.1 eV, which can be assigned to Hf $4f_{7/2}$ and Hf $4f_{5/2}$ spin states evidencing the formation of the HfO_2 bonds of the inorganic phase in the hybrid thin film [37,42]. In Fig. 3 (b), the O 1s core level spectrum has been deconvoluted into three major peaks located at 529.9 eV, 531 eV and 532.4 eV, respectively. The low intensity peak at 529.9 eV is related to oxygen species in the HfO_2 bonds [42], and the high intensity predominant peak at 531 eV is allotted to

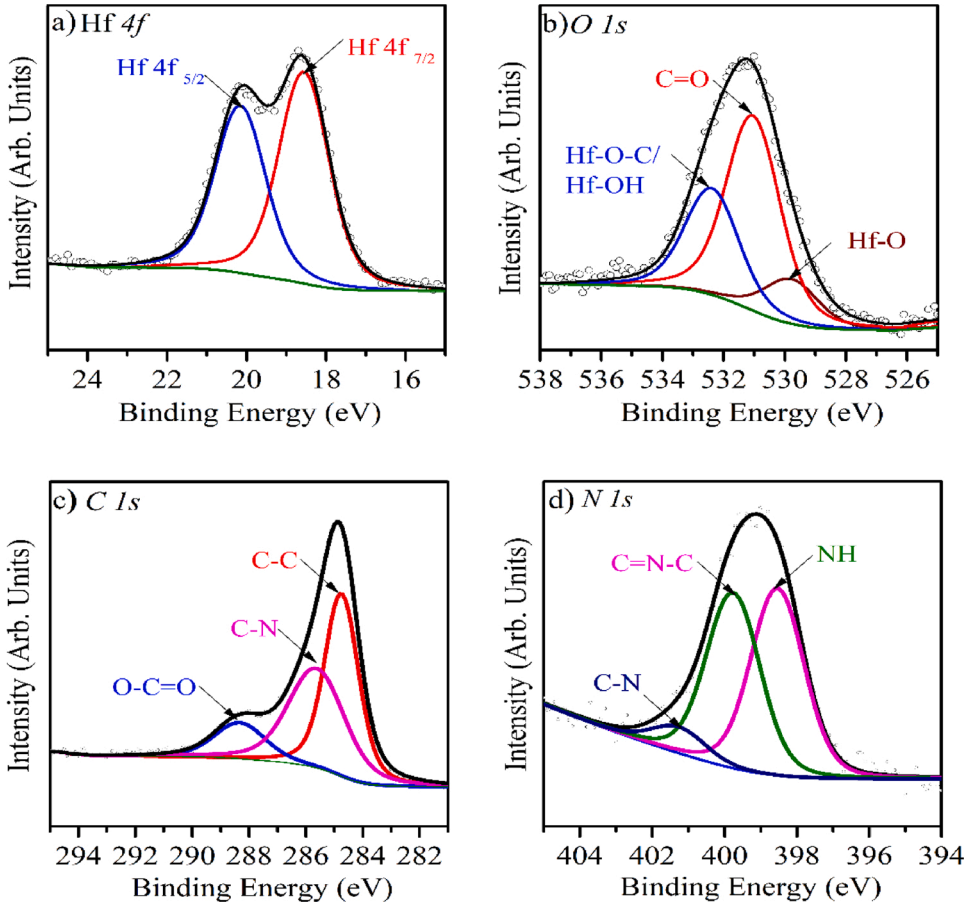

Fig. 3. XPS deconvolution spectra of solution processed HfO_2-PVP hybrid thin films (a) Hf 4f (b) O 1s (c) C 1s (d) N 1s.

C═O bond consistent to c-PVP polymer [33]. On the other hand, the intense peak at 532.4 eV was assigned to oxygen in Hf-O-C bonds, which is signaling the formation of a strong covalent chemical bond via thermal crosslinking process to join both inorganic and organic molecules in the hybrid network [37,41], or likely to be unreacted phenolic hydroxyl groups (−OH) bonded with inorganic hafnium molecules in the form of Hf−OH bonds [33,37]. The C1 s spectrum in Fig. 3 (c) shows the deconvolution into three peaks at 284.7 eV, 285.6 eV and 288.3 eV, respectively. These peaks were assigned to carbon species in C—C, C—N and O—C═O bonds, respectively, which are in the PVP polymer molecules and confirm the interaction of PVP with PMF cross-linker in the hybrid film [40,43]. Fig. 3 (d) shows the N 1s spectrum, which was deconvoluted into three peaks at the binding energies of 398.5 eV, 399.7 eV and 401.1 eV, respectively. The peaks are assigned to N—H, C═N and C—N, which are nitrogen groups in the PMF cross-linker molecules [36,40]. Based on these XPS results it can be concluded that the inorganic and organic phases develop strong covalent bonds connecting them in the hybrid network. This agrees with the FTIR analysis. Therefore, the hybrid structural characteristics are expected to improve the surface and dielectric properties of the hybrid layers for their utilization in the fabrication of TFTs.

3.2. Thermal analysis of the hybrid films

In order to explore the thermal stability of the HfO_2-PVP hybrid material, TGA analysis was performed in air atmosphere to get the information of the organic phase decomposition. The TGA curve of the hybrid material is shown in Fig. 4, where three different weight losses taking place in different temperature ranges are clearly observed. The first small weight loss of around 4% occurred at lower temperature, in the 25−190 °C temperature range. This can be due to the extraction of solvents, moisture and adsorbed water and hydroxyl groups still remaining in the hybrid material. Also, this weight loss has some contribution from the elimination of the unreacted phenolic groups (OH) contained in the PVP polymer. Later, the second weight loss of around 32 % is observed in the temperature region from 250 °C to 600 °C. This is the major weight loss originated from the degradation of PVP polymer and the trapped organic solvents in the hybrid network. At higher temperature, no negligible weight loss was identified, which suggests that the polymer decomposition is finalized and that the 64 % remaining material at the highest temperature is the amount of inorganic phase HfO_2 in the hybrid material.

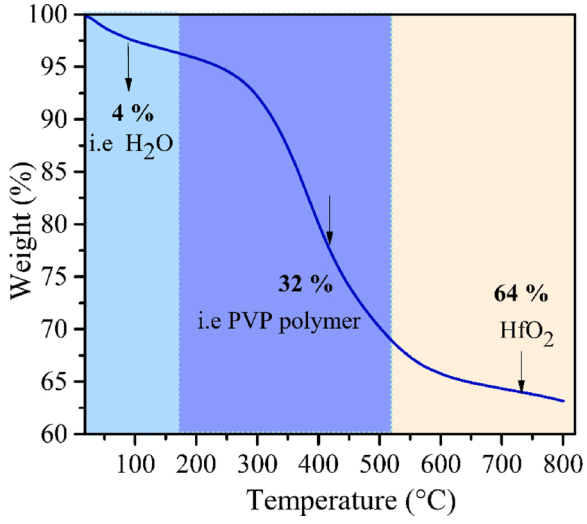

Fig. 4. Thermogravimetric analysis of the HfO_2-PVP hybrid dielectric material.

3.3. Hybrid dielectric morphology and surface energy

The surface roughness of hybrid dielectric thin films has been measured by atomic force microscopy (AFM). As shown in Fig. 5 (a), the surface topography of the hybrid thin film exhibits uniform and smooth surface with very low RMS surface roughness of 0.7 nm, without pinholes or any other defect. The homogenous and low surface roughness of the hybrid films is accomplished by the suitable blending of inorganic and organic phases coupled with crosslinking molecules. This suggests that the hybrid surface comprises with strong covalent chemical bonds (e.g. Hf-O-C, C–H) and polar groups (OH) confirmed by the FTIR and XPS analysis. Furthermore, the surface energy of the hybrid thin films was determined from contact angle measurements by using water, ethelene glycol and diiodomethane as testing liquids. The results are shown in Fig. 5(b) (73.3°), (c) (57.1°) and (d) (48.2°) for the three test liquids, respectively and this indicates that the hybrid dielectric surface has less hydrophilic behavior, which is stable in high humidity environment. By using the geometric model equatation [36], the obtained dispersion (γ_s^d) and polar (γ_l^p) components of the surface energies and the surface free energy (γ_S) of the crosslinked HfO_2-PVP hybrid thin film were 26.6 mJ m^{-2} and 10.1 mJ m^{-2} and 36.7 mJ m^{-2}, respectively. In fact, our estimated hybrid thin-film surface free energy is lower than that reported for other crosslinked PVP based polymer dielectrics [43]. This result suggests that the hybrid surface contains less polar groups, such as −OH groups, due to the successful crosslinking by PMF molecules with PVP polymer in a hybrid dielectric network. Compared with other dielectric surfaces, the low surface energy of the hybrid dielectrics offers an excellent growth conditions for solution based semiconductor layers especially for improving the interface properties [44,45]. The dielectric/semiconductor interface is very crucial for the device performance, by reducing the charge carrier traps in this region enables the achieving of high device mobility and reduction of hysteresis [45].

3.4. Electrical properties of HfO_2-PVP dielectric

Fig. 6 a) shows the scheme of the Metal-Insulator-Metal (MIM) capacitor structure, with Au/HfO_2-PVP/ ITO configuration, fabricated to determine the dielectric properties of the hybrid thin films with different inorganic volumetric ratios of 80/20, 60/40 and 20/80 (v/v %) of HfO_2-PVP. Among these,the best enhanced dielectrical properties were obtained by 60/40 composition and the obtained results were presented here. The other compositions results were shown in Fig. S1 and S2 respectively. In Fig. 6 b), the FE-SEM cross-section image of the hybrid dielectric film (60/40) shows its uniform thickness of 132 nm. Fig. 6 c) shows the leakage current density versus electric field (*J-E*) characteristics of the hybrid dielectric. Leakage current is one of the essential parameter to assess the reliability of a dielectric material for its implementation in electronic devices. As observed, the leakage current density varies from 1×10^{-8} to 1×10^{-10} A/cm^2 for an applied electric field -300 to 0 kV/cm. Particularly, the procured low leakage current may be attributed to the dense hybrid thin film with very smooth surface and low number of hydroxyl groups, as shown by AFM and contact angle measurements. The low leakage current density of the gate dielectric layer is highly essential for preventing the heat dissipation while device operating at higher voltages and to accomplish the low-off state currents in high-performance TFTs. The capacitance versus frequency (*C-f*) plots measured also in the same MIM device at different frequencies varying from 1 kHz to 1 MHz are shown in Fig. 6 d). It was found that the measured capacitance density of the 132 nm thick hybrid dielectric film decreased from 44.5 to 39.6 nF/cm^2 when the frequency increased from 1 kHz to 1 MHz. This slight drop of the hybrid dielectric layer capacitance of about 11 % is due to its different polarization mechanism, some of which have relatively slow polarization response and this frequency dispersion is corresponding to lack of slow polarization response at higher frequencies due to some organic impurities and the polarization

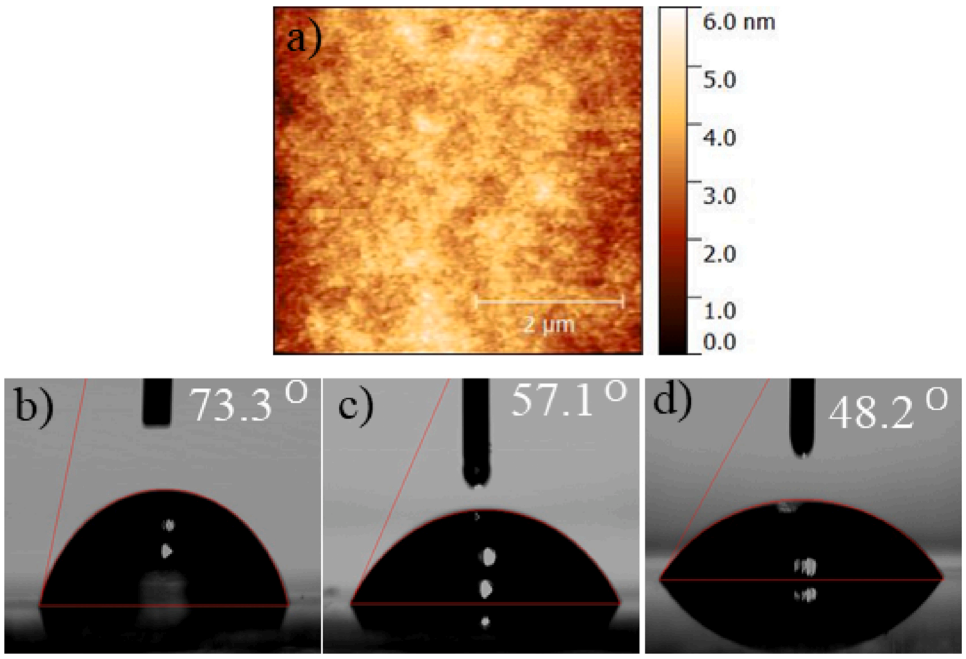

Fig. 5. Surface morphology of spin coated hybrid HfO_2-PVP dielectric thin-film of (a) 2D AFM topographic image and surface contact angle optical images of (b) water (c) ethylene glycol and (d) diiodomethane.

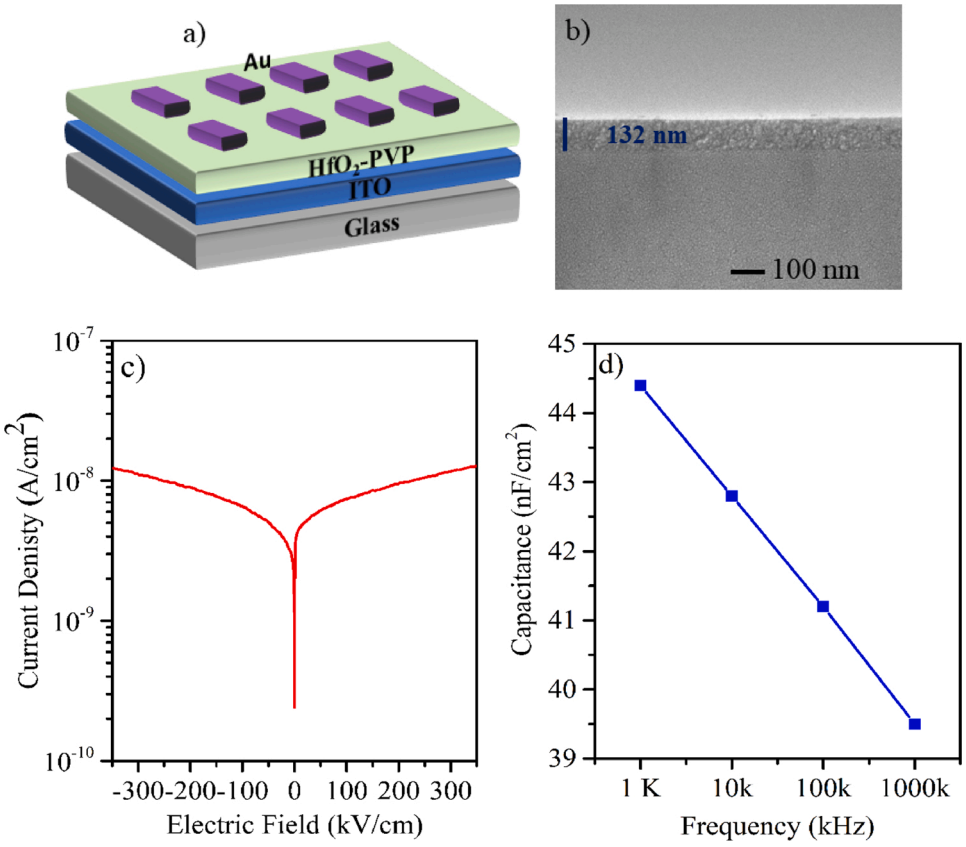

Fig. 6. a) Schematic of MIM capacitor structure, b) FESEM crossection image of HfO_2-PVP hybrid dielectric, c) *J-E* and d) *C-f* characteristics of HfO_2-PVP dielectric.

orientation in the hybrid thin films takes long time.The dielectric constant (*k*) of the hybrid dielectric film was determined from using a simple parallel plate capacitance equation and the thickness of the hybrid dielectric layer. The obtained dielectric constant values are 6.5, 6.3, 6.1 and 5.8 for 1 kHz, 10 kHz, 100 kHz, and 1 MHz, respectively. Finally, the obtained overall dielectric performance of the solution processed hybrid dielectric films in the MIM devices is highly favorable for gate dielectric applications in TFTs and the accomplished electrical parameters are equivalent to others reported for hafnium based hybrid dielectrics [31,33].

3.5. Electrical characterization of solution processed In2O3 TFTs

To examine the feasibility of the HfO_2-PVP hybrid thin films as gate dielectric layer, TFTs were fabricated integrating solution processed In_2O_3 as the n-type semiconductor channel layer. Fig. 7 a) depicts the schematic of the In_2O_3 TFT device assembled with bottom gate/top contacts architecture with width and length channel dimensions of W=100 μm and L=100 μm, respectively. Here, the In_2O_3 thin films engineered over the hybrid gate dielectric by solution process and deposited by low-cost efficient spin coating technique. Fig. 7 b) and c) show the atomic force microscope (AFM) surface morphologies of In_2O_3 channel layer surface deposited on the hybrid gate dielectric and annealed at two distinct temperatures of 200 °C and 230 °C, respectively. The measured surface RMS roughness of the In_2O_3 channel layers are 3.58 nm and 1.28 nm, respectively. The surface morphology of the semiconductor channel layer is crucial because it strongly affects the electron charge carrier transport in the channel layer and the charge traps at the electrical contacts/semiconductor interface of the devices [46]. The smoother surface of the In_2O_3 thin film annealed at higher temperature reveals its higher film densification, which is favorable to improve better electrical properties such as high electron mobilities (μ_{FE}), low threshold voltage (V_{TH}) and low subthreshold swing (SS).

The output curves of the In_2O_3-based TFTs with the different processing temperatures of 200 °C and 230 °C are shown in Fig. 8 a) and c), respectively. Both types of devices exhibit typical drain current (I_{DS}) versus source-drain voltage (V_{DS}) curves for n-channel conductivity, with linear behavior at low V_{DS} and saturating as V_{DS} increases. However, in particular, the output curves of the device with the channel layer processed at lower temperature suffers from the non linear ideal behavior at low V_{DS}, showing a shift to the right. As reported in literature, this effect is mainly caused by the high channel contact resistance at the electrical contacts/semiconductor channel interface [46]. Interestingly, this effect nullified in the output curves of the device with channel layer processed at 230 °C indicating the benefits of the higher temperature treatment. Also, the saturation drain currents measured at the highest source-drain voltage in this device increase about one order of magnitude as consequence of the lower contact resistance. On the other hand, Fig. 8 b) and d) show the typical transfer characteristic curves of both In_2O_3–based TFTs. In both cases, the source-drain current versus source-gate voltage curves (I_{DS}–V_{GS}) were measured in the current saturation region at V_{DS} = 10 and 4 V, respectively, in forward and reverse voltage scans. No hysteresis is observed between the forward and reverse scans which sense is indicated by the arrows in the graph..

At the lowest values of V_{GS}, the drain current is of the same order of 10^{-11} A in both devices, which is the off state current. At a low turn on voltage (Von) between 0 and 1 V in both devices, the drain current starts to increase exponentially tending to saturate at values of 10^{-7} A and 10^{-6} A at the highest V_{GS} values of 10 and 5 V, for the 200 °C and 230 °C-processed devices, respectively. These are the on state currents of the TFTs, which result in the on/off current ratio of the devices of the order of 10^4 and 10^5, respectively. The enhancement of the *on* state current and then of the *on/off* current ratio is produced by the annealing of the In_2O_3 channel layer at 230 °C, which improves its electrical and morphological properties and reduces the channel contact resistance. The field effect mobility in the saturation region and threshold voltage of both TFTs were calculated in the saturation region from the square root drain current versus gate voltage ($\sqrt{I_{DS}}$ -V_{GS}) plots (blue lines) by using the following Eq. 1:

$$\mu_{sat} = \frac{2L}{WC_G}\frac{d(\sqrt{I_{DS}})^2}{d(V_G)} \quad (1)$$

where μ_{sat} is the saturation mobility, L and W are the length and width of the TFT channel, C_G is the gate dielectric capacitance and $d\sqrt{I_{DS}}/dV_G$ represents the slope of the straight dashed line fitting the $\sqrt{I_{DS}}$-V_G experimental data. On the other hand, the linear fitting of the I_{DS} curve (red and black colour) determines the subthreshold swing (SS) values according to the following Eq. 2:

$$SS = (\partial(\log I_{DS})/(\partial V_G)) \quad (2)$$

The electrical parameters calculated for both types of devices are summarized in Table 1. As expected, the temperature treatment at 230 °C enhances the electrical performance of the TFTs, increasing their mobility from 0.08 to 2.6 cm^2/V.s, shifting the V_{TH} from negative, -0.9 V, (depletion mode) to positive, 0.1 V (enhancement mode), value and lowering the SS value from 770 to 330 mV/dec. The enhanced electrical performance of the In_2O_3 TFTs devices when the annealing temperature increased from 200 to 230 °C, is attributed to a higher formation degree of the In-O network established in the channel surface [10]. When the In_2O_3 film is processed at lower temperature, the film surface contributes a higher number of In−OH species, which tend to act as charge traps and degrades the device electrical properties. However, when the temperature increases, these hydroxyls groups are transformed into In-O bonds in the active layer increasing the film density and reducing the density of charge traps, which improved the electrical response of the TFTs. To analyze further the density of trap sites, we

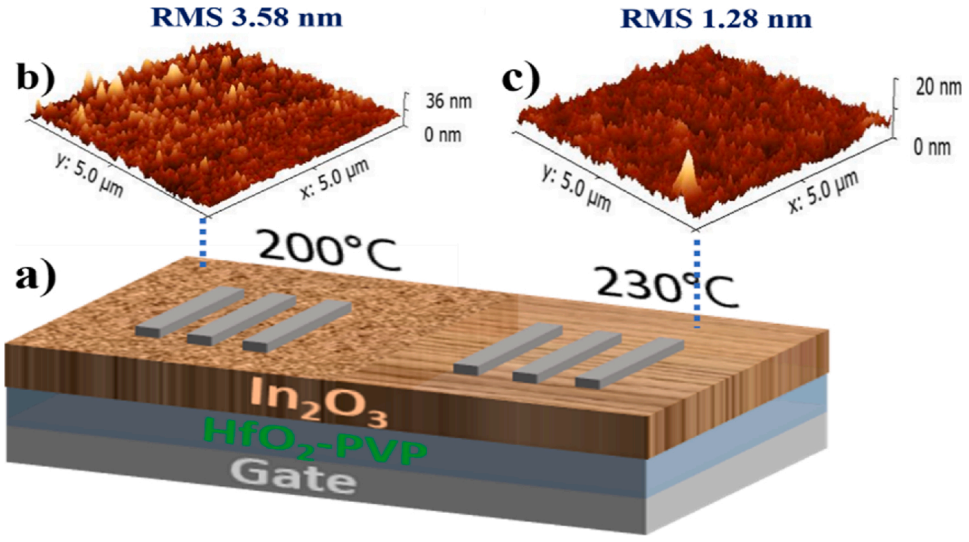

Fig. 7. a) Schematic of indium oxide (In_2O_3) TFT structure. AFM images of In_2O_3 channel layer morphology on HfO_2-PVP hybrid gate dielectric processed at b) 200 °C and c) 230 °C.

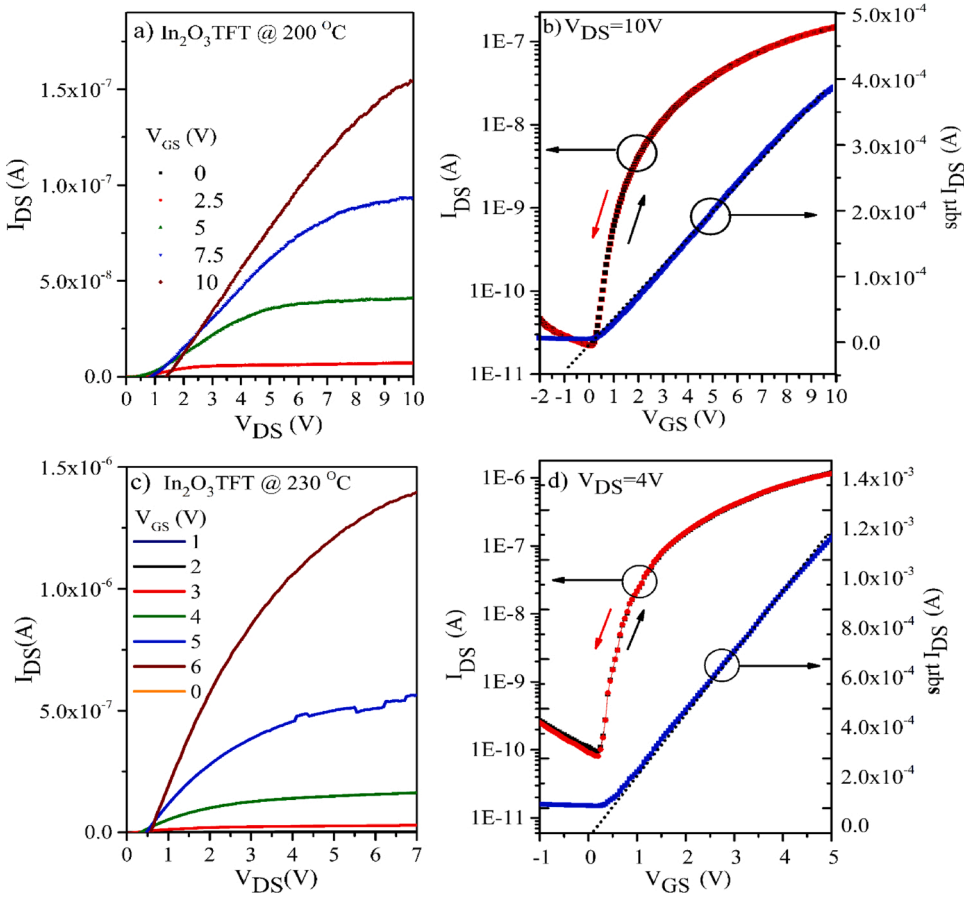

Fig. 8. Output curves of (a) 200 °C and (c) 230 °C and transfer curves of (b) 200 °C and (d) 230 °C In_2O_3 TFTs based on HfO_2-PVP hybrid dielectric.

Table 1
Electrical parameters of the In_2O_3 TFTs processed at 200 °C and 230 °C.

Temp °C	μ_{sat} (cm^2/Vs)	V_T (V)	I_{ON}/I_{OFF}	SS (mV/dec)	N_T (cm^2/eV)
200 °C	0.08	−0.9	10^4	770	3.3×10^{12}
230 °C	2.6	0.1	10^5	330	1.2×10^{12}

determined the number of traps at dielectric/semiconductor interface, N_T, from the following Eq. 3:

$$N_T = \left[\frac{SS\log(e)}{kT/q} - 1\right]\frac{C_i}{q} \quad (3)$$

where q is the electron charge, k is the Boltzmann constant, and T is the temperature. The computed values of N_T are 3.3×10^{12} and 1.2×10^{12} cm^2/eV for the 200 °C and 230 °C-processed devices, respectively. These values are also included in Table 1.The electrical parameters of obtained In_2O_3-based TFTs by using HfO_2-PVP hybrid gate dielectric are competing with those reported for thermally annealed at high temperature inorganic dielectrics [10,47–49].

4. Conclusions

In summary, we developed a novel inorganic-organic hybrid material using hafnium oxide (HfO_2) as the inorganic material and poly (vinylphenol) (PVP) as organic polymer material, synthesized via sol-gel method at a very low processing temperature under 200 °C. The obtained spin casted hybrid thin films are very homogeneous, smooth, and hydrophobic with a low surface energy, which is beneficial to achieve enhanced dielectric properties. The HfO_2-PVP hybrid thin films exhibited a low leakage current density ($\leq 10^{-9}$ A/cm^2 below 5 V) with dielectric constant (6.5 at 1 kHz). These desirable dielectric properties qualify the hybrids thin films for dielectric gate layers in complete solution processed In_2O_3TFTs, fabricated at low temperatures below 230 °C. The obtained complete solution based In_2O_3TFTs achieved low operating voltages with excellent electrical characteristics such as saturation electron mobility of 2.6 cm^2/V.s, I_{on}/I_{off} ratio of 10^5, threshold voltage of 0.1 V and subthreshold swing of 330 mV/dec, respectively. Therefore, these results indicate that the prepared hybrid dielectric thin films are potential candidates for future solution based high performance TFTs.

CRediT authorship contribution statement

M.G. Syamala Rao: Conceptualization, Writting - original draft, Writing - review & editing. **J. Meza-Arroyo:** Validation, Resources. **K. Chandra Sekhar Reddy:** Writing, Validation, Resources. **L.N.S. Murthy**: Results and discussion. **M.S. de Urquijo-Ventura:** Methodology, Writing - original draft, Resources. **F. Garibay-Martínez:** Methodology, Writing - original draft. **J.W.P. Hsu**: Manuscript revisison. **R. Ramirez-Bon:** Conceptualization, Supervision, Manuscript revision, Project administration.

Declaration of Competing Interest

The authors reported no declarations of interest.

Acknowledgements

The authors would like to acknowledge for the helpful technical support of Carlos Alberto Avila Herrera and the LIDTRA facilities. L.N.S. M. and J.W.P.H acknowledge the support of the National Science

FoundationCBET-1916612. J.W.P.H also acknowledges the Texas Instruments Distinguished Chair in Nanoelectronics.

Appendix A. Supplementary data

Supplementary material related to this article can be found, in the online version, at doi:https://doi.org/10.1016/j.mtcomm.2021.102120 .

References

[1] W. Xu, H. Li, J.-B. Xu, L. Wang, Recent advances of solution-processed metal oxide thin-film transistors, ACS Appl. Mater. Interfaces 10 (2018) 25878–25901, https://doi.org/10.1021/acsami.7b16010.

[2] H. Ling, S. Liu, Z. Zheng, F. Yan, Organic flexible electronics, Small Methods 2 (2018), 1800070, https://doi.org/10.1002/smtd.201800070.

[3] R. Chen, L. Lan, Solution-processed metal-oxide thin-film transistors: a review of recent developments, Nanotechnology. 30 (2019), 312001, https://doi.org/10.1088/1361-6528/ab1860.

[4] K.M. Jung, J. Oh, H.E. Kim, A. Schuck, K.R. Kim, K.C. Park, J.H. Jeon, S.Y. Lee, Y. S. Kim, Stability improvement of solution-processed IGZO TFTs by fluorine diffusion from a CYTOP passivation layer, J. Phys. D Appl. Phys. 53 (2020), https://doi.org/10.1088/1361-6463/ab8e7d.

[5] M.M. Islam, J.K. Saha, R.N. Bukke, M.M. Hasan, M.M. Billah, N.N. Mude, A. Ali, J. Jang, Solution-processed La alloyed ZrOx High-k dielectric for high-performance ZnO thin-film transistors, IEEE Electron Device Lett. 41 (2020), https://doi.org/10.1109/LED.2020.2992264, 1–1.

[6] A. Sharma, N.K. Chourasia, N. Pal, S. Biring, B.N. Pal, Role of Electron donation of TiO_2 gate interface for developing solution-processed high-performance one-volt metal-oxide thin-film transistor using ion-conducting gate dielectric, J. Phys. Chem. C. 123 (2019) 20278–20286, https://doi.org/10.1021/acs.jpcc.9b04045.

[7] Y. Zhou, J. Li, Y. Yang, Q. Chen, J. Zhang, Artificial synapse emulated through fully aqueous solution-processed low-voltage In_2O_3 thin-film transistor with Gd_2O_3 solid electrolyte, ACS Appl. Mater. Interfaces 12 (2020) 980–988, https://doi.org/10.1021/acsami.9b14456.

[8] X. Yu, J. Smith, N. Zhou, L. Zeng, P. Guo, Y. Xia, A. Alvarez, S. Aghion, H. Lin, J. Yu, R.P.H. Chang, M.J. Bedzyk, R. Ferragut, T.J. Marks, A. Facchetti, Spray-combustion synthesis: efficient solution route to high-performance oxide transistors, Proc. Natl. Acad. Sci. 112 (2015) 3217–3222, https://doi.org/10.1073/pnas.1501548112.

[9] D. Jiang, J. Li, W. Fu, Q. Chen, Y. Yang, Y. Zhou, J. Zhang, Light-stimulated artificial synapse with memory and learning functions by utilizing an aqueous solution-processed $In2O_3$ /AlLiO thin-film transistor, ACS Appl. Electron. Mater. 2 (2020) 2772–2779, https://doi.org/10.1021/acsaelm.0c00474.

[10] T.B. Daunis, J.M.H. Tran, J.W.P. Hsu, Effects of environmental water absorption by solution-deposited Al_2O_3 gate dielectrics on thin film transistor performance and mobility, ACS Appl. Mater. Interfaces 10 (2018) 39435–39440, https://doi.org/10.1021/acsami.8b15592.

[11] T.B. Daunis, D. Barrera, G. Gutierrez-Heredia, O. Rodriguez-Lopez, J. Wang, W. E. Voit, J.W.P. Hsu, Solution-processed oxide thin film transistors on shape memory polymer enabled by photochemical self-patterning, J. Mater. Res. 33 (2018) 2454–2462, https://doi.org/10.1557/jmr.2018.296.

[12] H. Wang, J. He, Y. Xu, N. André, Y. Zeng, D. Flandre, L. Liao, G. Li, Impact of hydrogen dopant incorporation on InGaZnO, ZnO and In_2O_3 thin film transistors, Phys. Chem. Chem. Phys. 22 (2020) 1591–1597, https://doi.org/10.1039/c9cp05050g.

[13] A.R. Kirmani, E.F. Roe, C.M. Stafford, L.J. Richter, Role of the electronically-active amorphous state in low-temperature processed In_2O_3 thin-film transistors, Mater. Adv. 1 (2020) 167–176, https://doi.org/10.1039/d0ma00072h.

[14] F. Jaehnike, D.V. Pham, R. Anselmann, C. Bock, U. Kunze, High-quality solution-processed silicon oxide gate dielectric applied on indium oxide based thin-film transistors, ACS Appl. Mater. Interfaces 7 (2015) 14011–14017, https://doi.org/10.1021/acsami.5b03105.

[15] P. Harishsenthil, J. Chandrasekaran, R. Marnadu, P. Balraju, C. Mahendarn, Influence of high dielectric HfO_2 thin films on the electrical properties of Al/HfO_2/n-Si (MIS) structured Schottky barrier diodes, Phys. B Condens. Matter. 594 (2020), 412336, https://doi.org/10.1016/j.physb.2020.412336.

[16] T.B. Daunis, K.A. Schroder, J.W.P. Hsu, Photonic curing of solution-deposited ZrO_2 dielectric on PEN: a path towards high-throughput processing of oxide electronics, Npj Flex. Electron. 4 (2020), https://doi.org/10.1038/s41528-020-0070-4.

[17] Q. Liu, C. Zhao, I.Z. Mitrovic, W. Xu, L. Yang, C.Z. Zhao, Comproportionation reaction synthesis to realize high-performance water-induced metal-oxide thin-film transistors, Adv. Electron. Mater. 6 (2020), 2000072, https://doi.org/10.1002/aelm.202000072.

[18] W. Cai, J. Brownless, J. Zhang, H. Li, E. Tillotson, D.G. Hopkinson, S.J. Haigh, A. Song, Solution-processed HfOx for half-volt operation of InGaZnO thin-film transistors, ACS Appl. Electron. Mater. 1 (2019) 1581–1589, https://doi.org/10.1021/acsaelm.9b00325.

[19] J. Weng, W. Chen, W. Xia, J. Zhang, Y. Jiang, G. Zhu, Low-temperature solution-based fabrication of high-k HfO_2 dielectric thin films via combustion process, J. Solgel Sci. Technol. 81 (2017) 662–668, https://doi.org/10.1007/s10971-016-4231-9.

[20] G. Park, H. Yang, J.H. Lee, G. Lee, J. Kwak, U. Jeong, Polymer-assisted deposition of Al-Doped HfO_2 thin film with excellent dielectric properties, Adv. Mater. Interfaces 6 (2019), 1900588, https://doi.org/10.1002/admi.201900588.

[21] G. He, W. Li, Z. Sun, M. Zhang, X. Chen, Potential solution-induced HfAlO dielectrics and their applications in low-voltage-operating transistors and high-gain inverters, RSC Adv. 8 (2018) 36584–36595, https://doi.org/10.1039/C8RA07813K.

[22] A. Liu, Z. Guo, G. Liu, C. Zhu, H. Zhu, B. Shin, E. Fortunato, R. Martins, F. Shan, Redox chloride elimination reaction: facile solution route for indium-free, low-voltage, and high-performance transistors, Adv. Electron. Mater. 3 (2017), 1600513, https://doi.org/10.1002/aelm.201600513.

[23] W. Sun, J. Zhao, S. Chen, X. Guo, Q. Zhang, Thermally cross-linked polyvinyl alcohol as gate dielectrics for solution processing organic field-effect transistors, Synth. Met. 250 (2019) 73–78, https://doi.org/10.1016/j.synthmet.2019.03.003.

[24] J. Zou, H. Wang, Z. Shi, X. Hao, D. Yan, Z. Cui, Development of high- k polymer materials for use as a dielectric layer in the organic thin-film transistors, J. Phys. Chem. C. 123 (2019) 6438–6443, https://doi.org/10.1021/acs.jpcc.9b00682.

[25] D.-H. Kang, W.-Y. Choi, H. Woo, S. Jang, H.-Y. Park, J. Shim, J.-W. Choi, S. Kim, S. Jeon, S. Lee, J.-H. Park, Poly-4-vinylphenol (PVP) and poly(melamine-co-formaldehyde) (PMF)-Based atomic switching device and its application to logic gate circuits with low operating voltage, ACS Appl. Mater. Interfaces 9 (2017) 27073–27082, https://doi.org/10.1021/acsami.7b07549.

[26] C. Lu, W.-Y. Lee, C.-C. Shih, M.-Y. Wen, W.-C. Chen, Stretchable polymer dielectrics for low-voltage-Driven field-effect transistors, ACS Appl. Mater. Interfaces 9 (2017) 25522–25532, https://doi.org/10.1021/acsami.7b06765.

[27] H. Kwon, X. Tang, S. Shin, J. Hong, W. Jeong, Y. Jo, T.K. An, J. Lee, S.H. Kim, Facile photo-cross-linking system for polymeric gate dielectric materials toward solution-processed organic field-effect transistors: role of a cross-linker in various polymer types, ACS Appl. Mater. Interfaces 12 (2020) 30600–30615, https://doi.org/10.1021/acsami.0c04356.

[28] K.-S. Jang, D. Wee, Y.H. Kim, J. Kim, T. Ahn, J.-W. Ka, M.H. Yi, Surface modification of a polyimide gate insulator with an yttrium oxide interlayer for aqueous-solution-Processed ZnO thin-film transistors, Langmuir. 29 (2013) 7143–7150, https://doi.org/10.1021/la401356u.

[29] M.G. Syamala Rao, S. Meraz-Davila, M.A. Quevedo-Lopez, R. Ramirez-Bon, Complete solution-processed low-voltage hybrid CdS thin-film transistors with polyvinyl phenol as a gate dielectric, IEEE Electron Device Lett. 39 (2018) 703–706, https://doi.org/10.1109/LED.2018.2822180.

[30] C. Chen, H. Yang, Q. Yang, G. Chen, H. Chen, T. Guo, Low-temperature solution-processed flexible metal oxide thin-film transistors via laser annealing, J. Phys. D Appl. Phys. 52 (2019), https://doi.org/10.1088/1361-6463/ab2c51.

[31] H.J. Cho, D.-H. Lee, E.-K. Park, M.S. Kim, S.Y. Lee, K. Park, H. Choe, J.-H. Jeon, Y.-S. Kim, Solution-processed organic-inorganic hybrid gate insulator for complementary thin film transistor logic circuits, Thin Solid Films 673 (2019) 14–18, https://doi.org/10.1016/j.tsf.2019.01.025.

[32] M.G. Syamala Rao, M.A. Pacheco-Zuñiga, L.A. Garcia-Cerda, G. Gutiérrez-Heredia, J.A. Torres Ochoa, M.A. Quevedo López, R. Ramírez-Bon, Low-temperature sol-gel $ZrHfO_2$-PMMA hybrid dielectric thin-films for metal oxide TFTs, J. Non. Solids 502 (2018) 152–158, https://doi.org/10.1016/j.jnoncrysol.2018.08.014.

[33] J.S. Hur, J.O. Kim, H.A. Kim, J.K. Jeong, Stretchable polymer gate dielectric by ultraviolet-assisted hafnium oxide doping at low temperature for high-performance indium gallium tin oxide transistors, ACS Appl. Mater. Interfaces 11 (2019) 21675–21685, https://doi.org/10.1021/acsami.9b02935.

[34] J.O. Kim, J.S. Hur, D. Kim, B. Lee, J.M. Jung, H.A. Kim, U.J. Chung, S.H. Nam, Y. Hong, K. Park, J.K. Jeong, Network structure modification-enabled hybrid polymer dielectric film with zirconia for the stretchable transistor applications, Adv. Funct. Mater. 30 (2020), 1906647, https://doi.org/10.1002/adfm.201906647.

[35] J. Meza-Arroyo, M.G. Syamala Rao, I. Mejia, M.A. Quevedo- López, R. Ramírez-Bon, Low temperature processing of Al_2O_3-GPTMS-PMMA hybrid films with applications to high-performance ZnO thin-film transistors, Appl. Surf. Sci. 467–468 (2019) 456–461, https://doi.org/10.1016/j.apsusc.2018.10.170.

[36] M.S. de Urquijo-Ventura, M.G.S. Rao, S. Meraz-Davila, J.T.- Ochoa, M.A. Quevedo-Lopez, R. Ramirez-Bon, PVP-SiO_2 and PVP-TiO_2 hybrid films for dielectric gate applications in CdS-based thin film transistors, Polymer. 191 (2020), 122261, https://doi.org/10.1016/j.polymer.2020.122261.

[37] G.S.R. Mullapudi, G.A. Velazquez-Nevarez, C. Avila-Avendano, J.A. Torres-Ochoa, M.A. Quevedo-López, R. Ramírez-Bon, Low-temperature deposition of inorganic–organic HfO_2–PMMA hybrid gate dielectric layers for high-mobility ZnO thin-film transistors, ACS Appl. Electron. Mater. 1 (2019) 1003–1011, https://doi.org/10.1021/acsaelm.9b00175.

[38] B.G. Son, S.Y. Je, H.J. Kim, J.K. Jeong, Modification of a polymer gate insulator by zirconium oxide doping for low temperature, high performance indium zinc oxide transistors, RSC Adv. 4 (2014) 45742–45748, https://doi.org/10.1039/c4ra08548e.

[39] H.J. Cho, D.-H. Lee, E.-K. Park, M.S. Kim, S.Y. Lee, K. Park, H. Choe, J.-H. Jeon, Y.-S. Kim, Solution-processed organic-inorganic hybrid gate insulator for complementary thin film transistor logic circuits, Thin Solid Films 673 (2019) 14–18, https://doi.org/10.1016/j.tsf.2019.01.025.

[40] F. Yin, P. Peng, W. Mo, S. Chen, T. Xu, The preparation of a porous melamine-formaldehyde adsorbent grafted with polyethyleneimine and its CO_2 adsorption behavior, New J. Chem. 41 (2017) 5297–5304, https://doi.org/10.1039/c7nj00240h.

[41] G. Vescio, J. López-Vidrier, R. Leghrib, A. Cornet, A. Cirera, Flexible inkjet printed high-k HfO_2-based MIM capacitors, J. Mater. Chem. C Mater. Opt. Electron. Devices 4 (2016) 1804–1812, https://doi.org/10.1039/c5tc03307a.

[42] H. Hernández-Arriaga, E. López-Luna, E. Martínez-Guerra, M.M. Turrubiartes, A. G. Rodríguez, M.A. Vidal, Growth of HfO_2/TiO_2 nanolaminates by atomic layer deposition and HfO_2-TiO_2 by atomic partial layer deposition, J. Appl. Phys. 121 (2017), https://doi.org/10.1063/1.4975676.

[43] S.J. Kim, M. Jang, H.Y. Yang, J. Cho, H.S. Lim, H. Yang, J.A. Lim, Instantaneous pulsed-light cross-linking of a polymer gate dielectric for flexible organic thin-film transistors, ACS Appl. Mater. Interfaces 9 (2017) 11721–11731, https://doi.org/10.1021/acsami.6b14957.

[44] K. Kim, H.W. Song, K. Shin, S.H. Kim, C.E. Park, Photo-cross-linkable organic-inorganic hybrid gate dielectric for high performance organic thin film transistors, J. Phys. Chem. C. 120 (2016) 5790–5796, https://doi.org/10.1021/acs.jpcc.6b00213.

[45] K. Kim, H. Kim, S.H. Kim, C.E. Park, Fluorinated polymer-grafted organic dielectrics for organic field-effect transistors with low-voltage and electrical stability, Phys. Chem. Chem. Phys. 17 (2015) 16791–16797, https://doi.org/10.1039/c5cp01909e.

[46] S. Tong, J. Sun, J. Yang, Printed thin-film transistors: research from China, ACS Appl. Mater. Interfaces 10 (2018) 25902–25924, https://doi.org/10.1021/acsami.7b16413.

[47] J. Chung, Y.J. Tak, W.G. Kim, J.W. Park, T.S. Kim, J.H. Lim, H.J. Kim, Low-temperature fabrication of solution-processed hafnium oxide gate insulator films using a thermally purified solution process, J. Mater. Chem. C Mater. Opt. Electron. Devices 6 (2018) 4928–4935, https://doi.org/10.1039/c8tc00899j.

[48] L. Zhu, G. He, J. Lv, E. Fortunato, R. Martins, Fully solution-induced high performance indium oxide thin film transistors with ZrO: x high-k gate dielectrics, RSC Adv. 8 (2018) 16788–16799, https://doi.org/10.1039/c8ra02108b.

[49] X. Li, J. Cheng, Y. Gao, M. Li, D. Kuang, Y. Li, J. Xue, T. Zhang, Z. Yu, Impact of NH3 plasma treatment for solution-processed indium oxide thin-film transistors with low thermal budget, J. Alloys. Compd. 817 (2020), 152720, https://doi.org/10.1016/j.jallcom.2019.152720.